



1 Humic surface waters of frozen peat bogs (permafrost zone)
2 are highly resistant to bio- and photodegradation

3

4 Liudmila S. Shirokova^{1,2}, Artem V. Chupakov², Svetlana A. Zabelina²,
5 Natalia V. Neverova², Dahedrey Payandi-Rolland¹, Carole Causseraund¹,
6 Jan Karlsson³, Oleg S. Pokrovsky^{1,4*}

7

8 ¹ *Geoscience and Environment Toulouse, UMR 5563 CNRS, University of Toulouse, 14 Avenue*
9 *Edouard Belin, Toulouse 31400, France*

10 ² *Institute of Ecological Problems of the North, N. Laverov Federal Center for Integrated Arctic*
11 *Research, Nab Severnoi Dviny 23, Arkhangelsk 163000, Russia*

12 ³ *Climate Impacts Research Centre (CIRC), Department of Ecology and Environmental*
13 *Science, Umeå University, 901 87 Umeå, Sweden*

14 ⁴ *BIO-GEO-CLIM Laboratory, Tomsk State University, 35 Lenina Pr., Tomsk 634050, Russia*

15

16 *corresponding author email: oleg.pokrovsky@get.omp.eu

17 Key words: depression, stream, river, organic carbon, photolysis, respiration, palsa, permafrost

18

19

20

21 **Bullet points:**

- 22 • Low (< 10%) concentration of bio- and photo-degradable DOM in humic waters from
- 23 frozen peatlands, discontinuous /continuous permafrost zone
- 24 • Low importance of biodegradation and photolysis on DOC processing and CO₂ evasion
- 25 in surface waters of permafrost-affected peatland regions.
- 26 • The paradigm of the importance of photolysis and biodegradation in DOC processing
- 27 in surface waters from permafrost region is challenged for the case of frozen peatlands
- 28 • We hypothesize the peat porewater DOM processing and respiration of sediments as
- 29 main drivers of elevated pCO₂ concentration and emission in humic boreal waters of
- 30 frozen peat bogs.

31

32

33

34



35 **Abstract**

36 Bio- and photo-degradation of dissolved organic matter (DOM) is identified as dominant vector
37 of C cycle in boreal and high-latitude surface waters. In contrast to large number of studies of
38 humic waters from permafrost-free regions and oligotrophic waters from permafrost-bearing
39 regions, the bio- and photo-lability of DOM from humic surface waters of permafrost-bearing
40 regions has not been thoroughly evaluated. Following standardized methods, we measured
41 biodegradation (low, intermediate, high temperature) and photodegradation (one intermediate
42 temperature) of DOM in surface waters along the hydrological continuum (depression →
43 stream → thermokarst lake → river Pechora) within a European Russian frozen peatland. In all
44 systems, there was no measurable ($\geq 10\%$) bio- or photodegradation of DOM over 1 month of
45 incubation. It is possible that the main cause of the lack of degradation is the dominance of
46 allochthonous refractory (soil, peat) DOM in all studied waters. Yet, all surface waters were
47 supersaturated with CO₂. Thus, this study suggest that, rather than bio- and photo-degradation
48 of DOM in the water column, other factors such as peat porewater DOM processing and
49 respiration of sediments are the main drivers of elevated pCO₂ and emission in humic boreal
50 waters of frozen peat bogs.

51

52 **Introduction**

53 Boreal and subarctic waters contain large amounts of plant, soil, and peat-originated
54 dissolved organic matter (Wilkinson et al., 2013; Kaiser et al., 2017), and the proportion of
55 land-derived organic carbon in waters is likely to increase with ongoing permafrost thaw
56 (Wauthy et al., 2018). Heterotrophic bacteria degrade this DOM (Karlsson, 2007; McCallister
57 and del Giorgio, 2008), causing net heterotrophic conditions (Gross Primary Productivity <
58 Respiration) and CO₂ emission to the atmosphere from surface waters (Ask et al., 2012;
59 Lapierre et al., 2013). Between 10% and 40% of the dissolved organic carbon (DOC) in lakes,



60 rivers and soil waters of the boreal zone may be available for bacterial uptake over a time frame
61 of several weeks (Berggren et al., 2010; Roehm et al., 2009). The biodegradability of DOM
62 leached from permafrost and non-permafrost soils was recently reviewed by Vonk et al. (2015)
63 who concluded that aquatic DOC is more biodegradable in regions with continuous permafrost
64 compared to regions without permafrost. At the same time, among all Arctic rivers, the highest
65 annual (20%) and winter (ca. 45%) biodegradable DOC (BDOC) was reported for the Ob River,
66 draining through peatlands with minimal influence of permafrost (Wickland et al., 2012).
67 Further, based on 14 studies of BDOC and their own research, Vonk et al. (2015) demonstrated
68 zero BDOC loss in aquatic systems without permafrost, which is contradictory to general
69 understanding of biodegradation of aquatic DOM as major driver of CO₂ emission in boreal
70 waters. It is also important to note that all the available bio-degradation studies of inland waters
71 in permafrost regions dealt with either mountain regions with essentially mineral soil substrates
72 in Alaska or Canada (Holmes et al., 2008; Wickland et al., 2012; Ward et al., 2017) or with the
73 yedoma soils of Eastern Siberia (Mann et al., 2014, 2015; Spencer et al., 2015).

74 Similarly, although the photolysis of dissolved organic matter (DOM) in boreal and
75 subarctic aquatic environments contributes to CO₂ emission from the inland waters to the
76 atmosphere (Cory et al., 2014), the overwhelming majority of photo-degradation studies in the
77 Arctic were conducted on oligotrophic lake waters and streams draining mineral soils of
78 mountain regions (Ward and Cory, 2016; Cory et al., 2013, 2015). The dominance of photolytic
79 processes in DOM processing in arctic waters was reported for N America (Cory et al., 2014;
80 Ward et al., 2017), Canadian surface waters of the temperate zone (Winter et al., 2007; Porcal
81 et al., 2013, 2014, 2015), and small Swedish humic-rich headwater catchments (Köhler et al.,
82 2002). In contrast, several other studies from Scandinavia (Groeneveld et al., 2016; Koehler et
83 al., 2014), Canada (Laurion and Mladenov, 2013; Gareis and Lesack, 2018) and NW Russia
84 (Oleinikova et al., 2017; Chupakova et al., 2018) demonstrated sizeable removal of colored



85 (chromophoric DOM) but quite small ($\leq 10\%$) impact of sunlight irradiation on bulk DOC
86 concentration in streams, rivers and lakes.

87 The controversies in both bio- and photo-degradation capacity of surface waters from
88 the arctic regions described above clearly call a need for further studies of these processes,
89 encompassing wider range of aquatic settings. The numerous surface waters located within
90 discontinuous to continuous permafrost zone of Northern Eurasia, where most aquatic systems
91 are drained through frozen peat rather than mineral substrates, are poorly studied regarding bio-
92 and photo-degradability of aquatic DOM. Yet, these regions (NE European Russia or
93 Bolshezemelskaya tundra, Western Siberia Lowland, Northern Siberian Lowland, Kolyma and
94 Yana-Indigirka Lowland) occupy > 2 million km^2 which is more than 10% of overall
95 permafrost-affected land area and exhibit, in average, ten times higher concentration of soil
96 organic C in the form of 0.5 to 3 m thick peat layer than the rest of the circumpolar regions. As
97 a result of the dominance of histosols, the surface waters draining frozen peatlands are enriched
98 in DOC compared to other permafrost-affected regions (Manasypov et al., 2014; Pokrovsky et
99 al., 2015) and may provide disproportionately high contribution to overall DOM bio- and photo-
100 degradability in the Arctic and subarctic regions.

101 Numerous experiments in permafrost-bearing and permafrost-free aquatic environments
102 on mineral soil substrates relatively poor in DOC demonstrated that the headwater streams and
103 soil leachate contain most bio-degradable and photo-degradable DOM (Ilina et al., 2014; Mann
104 et al., 2014, 2015; Larouche et al., 2015; Spencer et al., 2015; Vonk et al., 2015). Thus, we
105 hypothesized that, given rather oligotrophic (nutrient-poor) nature of Sphagnum peat from
106 histosols, the bioavailability of essentially recalcitrant DOM in surface waters of frozen
107 peatlands will be low. However, we expected a gradient in the degree of bio- and photo-lability
108 of DOM from permafrost subsidence, head water stream, thermokarst lake and large river,
109 corresponding to the increase in water residence time (Mann et al., 2012).



110 To test these hypotheses, we used recommended standardized protocol for DOM
111 biodegradation (Vonk et al., 2015) and applied it for 4 main aquatic components of a
112 hydrological continuum ‘permafrost subsidence → small stream → large thermokarst lake →
113 large river (Pechora)’. We chose the largest frozen peatlands in Europe, the Bolshezemelskaya
114 Tundra of NE European Russia which is represented by flat-mound (palsa) peat bog
115 (discontinuous and continuous permafrost zone) and belongs to the watershed of the largest
116 European permafrost-affected river, Pechora. Specific questions of this study were (i) to assess
117 the difference in BDOC and photodegradable (PDOC) fraction of DOM in surface waters of
118 frozen peat bog along the hydrological continuum, from permafrost depression to large rivers,
119 (ii) to relate the BDOC and PDOC concentrations to the snapshot CO₂ concentration and
120 emission, and (iii) to quantify the impact of temperature on biodegradation potential of surface
121 waters from frozen peatbogs and predict possible impact of warming on DOM biodegradation
122 efficiency. We measured very low bio- and photo-degradability of aquatic DOM from frozen
123 Arctic peatland which may require revisiting the current paradigm of the importance of bio-
124 and photodegradation of DOC in permafrost regions; this should be taken into account for pan-
125 Arctic modeling of C biogeochemical cycle in continental waters.

126

127 2. Study site and methods

128 2.1. Geographical context and hydrological continuum of the Pechora River basin

129 The water samples were collected in the end of July 2017 within the BolsheZemelskaya
130 Tundra (BZT) peatland (continuous to discontinuous permafrost zone), which belongs to the
131 Pechora River watershed (**Fig. S1**), the largest European Arctic river draining permafrost-
132 bearing terrain (watershed = 322,000 km²; mean annual discharge is 4140 m³/s). The northern
133 part of the Pechora watershed is covered by permafrost: discontinuous on the eastern part and
134 sporadic to isolated on the western part (Brittain et al., 2009). The BZT is a hilly moraine



135 lowland located between rivers Pechora and Usa (from the west and south) and the Polar Ural
136 and Pai-Khoi ridge from the east. The dominant altitudes are between 100 and 150 m, created
137 by hills and moraine ridges, composed of sands and silt with boulders. Between the moraines
138 and ridges there are many lakes, mostly of thermokarst origin. The dominant soils are histosols
139 of peat bogs and podzol-gleys in the southern forest-tundra zone. The mean annual temperature
140 is -3.1°C and the mean annual precipitation is 503 mm. The dominant vegetation of the tundra
141 zone is mosses, lichens and dwarf shrubs.

142 We sampled surface waters along the typical hydrological continuum, consisting of 1)
143 depression in the moss and lichen cover of upland frozen peat bog, filled by water from thawing
144 of ground ice (permafrost subsidence, 2.5 x 3 m size and 0.3 m depth); 2) small stream (~2 km
145 length) originated from upland peat bog; 3) small thermokarst lake Isino ($S_{\text{area}} = 0.005 \text{ km}^2$)
146 located within the peat bog, and 4) the Pechora River mainstream. Similar principle of the
147 hydrological continuum was considered in the Kolyma River biodegradation experiments
148 (Mann et al., 2012). The list of sampled water objects together with their physical, chemical
149 characteristics and parameters of CO_2 system is presented in **Table 1**. The surface waters were
150 collected from the shore (depression and stream) or the PVC boat (r. Pechora and Lake Isino).
151 The water samples were placed into 2-L Milli-Q pre-cleaned PVC jars and kept refrigerated
152 until arrival to the laboratory, within 2-3 h after collection.

153

154 *2.2. Experimental set-up*

155 2.2.1. Biodegradation

156 For biodegradation assays we followed the standardized protocol for assessing
157 biodegradable DOC of Arctic waters (Vonk et al., 2015). To facilitate the implementation of
158 recommended protocol, we used exactly the same filter towers, inline filter holders, and vacuum
159 devices as depicted in Vonk et al. (2015). Initial samples were filtered through pre-combusted



160 (4.5 h at 450°C) Whatman GF/F filters of nominal poresize 0.7 μm . All the manipulations were
161 performed in laminar hood box (class A100) under sterile environment; the working space was
162 sterilized by UV light before preparation. Triplicate 30 mL aliquots of 0.7 μm -filtered water
163 were placed into pre-combusted (4.5 h at 450°C) dark borosilicate glass bottles of 40 mL
164 volume, without nutrient amendment and stored at $23\pm 1^\circ\text{C}$ in the dark in thermostat. The bottles
165 were closed with sterilized PVC caps. As recommended, the caps were left loose and the bottles
166 were shaken manually once a day avoiding the liquid touching the cap. The incubated samples
167 were re-filtered through pre-combusted 0.7 μm GF/F filters using sterilized dismountable
168 Sartorius 25 mm filter holder and a cleaned sterile syringe after 0, 2, 7, 14 and 28 days of
169 exposure. All handling and sampling of bottles was performed in the laminar hood box under
170 sterilized workspace. Filtered samples were acidified with 30 μL of concentrated (8.1 M)
171 double distilled HCl, tightly capped and stored in the refrigerator between 1 and 2 month before
172 DOC analyses. Non-acidified portion of filtrate was used for pH, Specific Conductivity, DIC
173 and $\text{UV}_{254\text{ nm}}$ and optical spectra measurement. Control runs were 0.22 μm sterile-filtered water
174 which was incubated in parallel to experiments and re-filtered through 0.7 μm GF/F filters at
175 the day of sampling.

176 In addition to this ‘classic’ protocol, we used alternative procedure of biodegradation
177 experiments to test maximally possible DOM removal by bacteria. For this, we replaced initial
178 0.7 μm GF/F filtration by 3 μm filtration through sterilized Nylon Sartorius membranes, to
179 increase the amount of bacterial cells capable to degrade DOM during incubation. The reason
180 for that is that conventional 0.7 μm (GF/F) filtration might remove too many microbial cells.
181 Besides, re-filtration through the same filter pore size (0.7 μm) recommended in classic protocol
182 may not necessarily remove the newly formed microbial biomass as the cell size of bacteria
183 grown during incubation may not exceed 0.7 μm . In this regard, initial 3 μm -filtration is
184 equivalent of 100% inoculum used by Vonk et al. (2015) and can be considered as maximal



185 enhancement of DOM biodegradation without addition of nutrients. Further, instead of 0.7 μm
186 refiltration for sampling, we employed 0.22 μm filter pore size for DOC samplings during
187 incubation. This allowed to remove all particulate organic carbon formed via microbial
188 metabolism, as well as some newly grown microbial cells and therefore should enhance the
189 degree of biodegradation calculated as the difference between initial 3 μm -filtration and 0.22
190 μm filtration at the date of sampling. The control runs were filtered through sterile 0.22 μm
191 filters and incubated parallel to the experiments, following the standard approach for control
192 abiotic experiments in incubation experiments (Köhler et al., 2002). They were re-filtered
193 through 0.22 μm membrane at the day of experimental sampling. To insure the lack of DOC
194 release from sterilized Nylon membrane, we run blank (Milli-Q) filtration through both 0.7 μm
195 GF/F and 0.22 μm Nylon filters; in both cases the DOC blank was below 0.1-0.2 mg/L which
196 is less than 1% of DOC concentration in our samples. The glass bottles were incubated in
197 triplicates at $4\pm 2^\circ\text{C}$, $22\pm 1^\circ\text{C}$ and $37\pm 3^\circ\text{C}$ using refrigerator and incubators and agitated
198 manually at least once a day over 4 weeks of exposure.

199

200 2.2.2. Photodegradation

201 For photodegradation incubations, water samples of all sites except the river were
202 collected in polypropylene jars and sterile filtered (0.22 μm Nalgene Rapid-Flow Sterile
203 Systems) within 2 h of sampling and refrigerated. Note that the 0.22 μm sterile filtration is the
204 only way of conducting photodegradation experiments, given that the autoclave sterilization of
205 DOM-rich natural water would coagulate humic material and thus is not suitable (Andresson et
206 al., 2018). In this regard, we followed conventional methodology in this field which is exposure
207 of 0.2 μm -sterile filtered samples in quartz reactors in the outdoor pool (Vähätalo et al., 2003;
208 Chupakova et al., 2018; Gareis and Lesack, 2018), solar simulator (Lou and Xie, 2006; Amado
209 et al., 2014) or directly in the lake water (Laurion and Mladenov, 2013; Groeneveld et al., 2016).



210 The filtrates were transferred under laminar hood box into sterilized, acid-washed quartz tubes
211 (150 mL volume, 20% air headspace) and placed at 3 ± 2 cm depth into outdoor pool which was
212 filled by river water having the light transparency similar to that of the Pechora River (1.5-2.0
213 m Secchi depth). In-situ measurements of sunlight intensity were conducted using submersible
214 sunlight sensor. The outdoor pools were placed under unshaded area, at the latitude similar to
215 that of the sampling sites. Slight wind movement and regular manual shaking allowed for
216 sufficient mixing of the interior of reactors during exposure. All the experiments were run in
217 triplicates. The water temperature was $19\pm 3^\circ\text{C}$ over 28 days of exposure (18 July - 8 August),
218 with an average magnitude of diurnal water temperature variation of 6°C (recorded every 3 h
219 using EBRO EBI 20 Series loggers). The day light intensity was typically between 5,000 and
220 20,000 lux (in average 10,000 lux or 14 ± 5 W/m²) which is within the range of solar radiation
221 at the latitude of the polar circle in the end of July - beginning of August. We have chosen 4
222 weeks exposure time for consistency with biodegradation experiments described above and
223 following the previous studies on photodegradation under sunlight, which is typically from 15
224 to 70 days (Moran et al., 2000; Vähätalo and Wetzel, 2004; Mostofa et al., 2007; Helms et al.,
225 2008; Chupakova et al., 2018). Dark control experiments were conducted in duplicates, using
226 sterilized glass tubes filled by sterile 0.22 μm -filtered water, wrapped in Al foil and placed in
227 the same outdoor pool as the experiments. The headspace (approx. 20% of total reaction
228 volume) was similar in experimental and control reactors. The individual reactors were sterile
229 sampled at the beginning and at the 2nd, 7th, 14th, 21th and 28th day of exposure. Each sampling
230 sacrificed the entire reactor. The MilliQ blanks were collected and processed to monitor for any
231 potential sample contamination introduced by our filtration, incubation, handling and sampling
232 procedures. The organic carbon blanks of filtrates never exceeded 0.2 mg/L.

233

234

235 2.3. *Analyses and treatment*

236 The temperature, pH, O₂ and specific conductivity in surface waters were measured in
237 the field as described previously (Shirokova et al., 2013b). Dissolved CO₂ concentration was
238 measured using portable submersible Vaissala Carbocap® GM70 Hand-held carbon dioxide
239 meter with GMP222 probes (accuracy 1.5%). The diffusional CO₂ flux was calculated using
240 wind-based model (Cole and Caraco, 1998) with $k_{600} = 2.07 + 0.215 \times u_{10}^{1.7}$, where u_{10} is the wind
241 speed at 10 m height. In the filtrates, we measured optical density at 254 nm and at selected
242 wavelengths (365, 436 and 470 nm) of the visible spectrum, the concentration of dissolved
243 organic and inorganic carbon (DOC and DIC, respectively). The DOC and DIC were analyzed
244 by high-temperature catalytic oxidation using TOC-VCSN, Shimadzu® (uncertainty ± 2%, 0.1
245 mg L⁻¹ detection limit). The DIC was measured after sample acidification with HCl and DOC
246 was analyzed in acidified samples after sparging it with C-free air for 3 min at 100 mL min⁻¹ as
247 non-purgable organic carbon (NPOC). Selected quartz reactors in photodegradation
248 experiments were used to measure dissolved O₂ using Oxi 197i oximeter with a Cellox® 325
249 galvanic submersible sensor (WTW, Germany; ± 0.5% uncertainty). For this, the O₂ galvanic
250 sensor was introduced into the quartz tube immediately after opening of the reactor and allowed
251 to equilibrate for 5-10 min while protecting the open end of the tube from the exchange with
252 atmospheric oxygen via wrapping it in Al foil. All filtered samples collected from photo-
253 degradation experiments were acidified with ultrapure nitric acid and analyzed for major and
254 trace elements following procedures employed in GET (Toulouse) for analyses of boreal humic
255 waters (Oleinikova et al., 2017, 2018).

256 To account for possible microbial development in biodegradation experiments, we
257 performed oligotrophic and eutrophic bacteria count in the course of incubation, following the
258 standard methodology used in biodegradation experiments of peat waters (Stutter et al., 2013)
259 as also described previously (Shirokova et al., 2017b; Chupakova et al., 2018). In addition, we



260 measured total bacterial number and quantified the dominant cell size morphology using DAPI
261 fluorescence method (Porter and Feig, 1980). Control experiments did not demonstrate the
262 presence of any countable cells in the observation fields.

263 The bio- and photodegradable DOC (BDOC and PDOC, respectively) were calculated
264 in percent loss relative to control at each sampling time point t (0, 2, 7, 14 and 28 days)
265 according to:

$$266 \quad \text{BDOC}(\%)_t = 100\% \times (\text{DOC}_{t, \text{control}} - \text{DOC}_t) / \text{DOC}_{t, \text{control}} \quad (1)$$

267 Alternatively, the BDOC and PDOC were calculated in percent loss at time point t relative to
268 the initial concentration of DOC ($\text{DOC}_{t=0}$) following Vonk et al. (2015):

$$269 \quad \text{BDOC}(\%)_t = 100\% \times (\text{DOC}_{t=0} - \text{DOC}_t) / \text{DOC}_{t=0} \quad (2)$$

270 For most treatments and sampled waters, the difference between two methods of bio-
271 /photodegradable DOC concentration was statistically negligible. Note that in case of negative
272 values provided by Eqn. 2, the BDOC was taken as 0% following the conventional practice in
273 biodegradation experiments (Vonk et al., 2015). The uncertainties of BDOC % numbers were
274 between ± 5 and $\pm 10\%$ for experiments, at 4, 23 and 37°C using modified (3 μm and 0.22 μm
275 filtration) protocol. In ‘classic’ protocol (0.7 μm GF/F filtration) the uncertainties were as high
276 as 15-20% at the end of experiment. We believe that such high uncertainties are linked to high
277 initial DOC concentration, triplicate measurements and simultaneous monitoring of
278 experimental and control runs.

279 Statistical treatment included the least squares method and the Pearson correlation,
280 because the data were normally distributed. The ANOVA method was used to test the
281 differences in the average DOC concentration versus time in incubation experiments and in the
282 controls and to assess the difference between the light experiments and the dark control for
283 photo-degradation experiments.

284



285 **3. Results**

286 *3.1. Assessment of biodegradable DOC*

287 The waters of hydrological continuum within the Pechora River basin are highly diverse
288 (**Table 1**), with pH range from 3.8 (frozen peat depression) to 6.9 (r. Pechora). The soluble salts
289 concentrations are low as the specific conductivity ranged from $20 \pm 10 \mu\text{S cm}^{-1}$ (stream,
290 thermokarst lake) to $\sim 60 \mu\text{S cm}^{-1}$ in the peat bog depression and the Pechora River. The DOC
291 concentration decreased from 44 mg/L in frozen peat depression to ~ 8 mg/L in the Pechora
292 River following the order of water residence time (flow direction) “depression \gg stream \geq
293 thermokarst lake $>$ r. Pechora”. The DOC concentration was generally similar (within $\pm 2\%$)
294 between 3, 0.7 and 0.22 μm pore size filtration of the initial sample, in agreement with former
295 size fractionation measurement in Arctic and subarctic systems (Vasyukova et al., 2010;
296 Pokrovsky et al., 2012, 2016). All sampled surface waters exhibited CO_2 supersaturation with
297 respect to atmosphere (from 440 to 2400 ppm) and net CO_2 emission (diffusion) flux ranging
298 from 34 to 74 $\text{mmol CO}_2 \text{ m}^{-2} \text{ d}^{-1}$ (**Table 1**).

299 In both protocols of biodegradation experiments, two major features were noted: (1) the
300 concentrations of 0.7 μm and 0.22 μm -filtered DOC did not decrease during the exposure and
301 (2) there was no sizable ($> 10\%$) difference between the control run and the incubation
302 experiment (**Fig. 1**). By ‘classic’ protocol of biodegradation experiments (0.7 μm GF/F
303 filtration) at 23°C, the BDOC fraction ranged between 0 and 10 % for all surface waters. The
304 modified procedure (3 μm initial filtration and 0.22 μm sampling) did not detect any significant
305 biodegradation for any of the studied waters (average equaled to $5 \pm 5\%$ at 4, 23 and 37°C, **Fig.**
306 **2 B, C, D**). The DIC concentrations increased only in stream water incubated at 37°C, where
307 we measured $\sim 10\%$ increase over 28 days of exposure (not shown). This increase was equal to
308 0.2 mg/L of DIC. Note that equivalent decrease in DOC concentration could not be assessed,



309 presumably due to high DOC concentration (17 mg/L) and the intrinsic uncertainty on NPOC
310 analyses (2%) which did not allow measuring C change smaller than 0.3 mg/L.

311 The $UV_{254\text{ nm}}$ absorbency of samples in the course of dark aerobic exposure
312 demonstrated slight decrease with time (ca., between 5 and 10% over 28 days) in peat bog
313 depression by ‘classic’ protocol (**Fig. S2 of Supplement**). However, in all other treatments, the
314 control was indistinguishable from experimental runs and the $SUVA_{254}$ remained constant
315 within the uncertainties of triplicates (ca., ± 5 to $\pm 10\%$).

316 The microbial consortium of all systems was dominated by cocci (0.23 μm median size)
317 and rods (0.96 x 0.20 μm) as revealed from DAPI fluorescent imaging. The number of
318 culturable oligotrophic bacteria increased by a factor of ~ 100 after first 2-7 days of exposure
319 at 23°C both in GF/F-filtered and 3 μm -filtered samples, and then remained stable at ca. 10,000
320 to 20,000 CFU mL^{-1} till the end of experiments (**Fig. S3 A, C**). The highest concentration of
321 oligotrophic bacteria was observed in the Pechora River, where as the other samples were not
322 significantly different between each other. The CFU value at 4°C ranged between 1000 and
323 5000 CFU mL^{-1} and did not demonstrate any clear pattern with time of incubation (**Fig. S3 B**).
324 The number of eutrophic bacteria ranged between 1,000 and 15,000 CFU mL^{-1} following the
325 order: r. Pechora > stream \geq peat bog depression \geq thermokarst lake. There was no growth of
326 eutrophic or oligotrophic bacteria at 37°C. The total cell number gradually increased in the
327 course of experiment at 23°C with maximal changes observed in peatbog depression and the
328 Pechora River (**Fig. S3 D**). There was a progressive increase of rod-shaped bacillus relative to
329 coccus in the Pechora River and a permafrost stream whereas the thermokarst lake and peatbog
330 depression did no exhibit any systematic change in dominant bacteria morphologies during the
331 biodegradation experiments.

332

333



334 3.2. Photodegradation of DOM from frozen peatlands

335 The pH of exposed samples did not exhibit any systematic variation within 0.5 pH unit.

336 The DIC remained fairly stable (within 0.5 mg/L) without any significant ($R^2 < 0.5$; $p > 0.05$)
337 change during incubation, regardless of the type of system, DOC and DIC concentration (not
338 shown). The exposed water remained oxygenated (average O_2 saturation close to 90%) with no
339 detectable change (i.e. $> 10\%$) over the course of experiment. Specific conductivity also
340 remained highly stable over full period of exposure.

341 The bacteria count in photo-degradation reactors at the beginning of exposure and after
342 14 and 28 days of incubation yielded between 1 and 100 CFU mL^{-1} . This is a factor of 100 to
343 1000 lower than the number of cells in experiments of bio-degradation run in non-sterilized
344 waters over the same duration of experiments (section 3.1). As such, the microbial degradation
345 was considered negligible at our experimental conditions.

346 There was no sizeable decrease in DOC concentration during 28 d of exposure to
347 sunlight (**Fig. 3 A**). This relative change of DOC concentration ranged from -5 % to +5 % and
348 it did not exceed the non-systematic variability among triplicates. Although the triplicate agreed
349 within less than 2 % (the symbol size in **Fig. 3**), the small change of DOC in peat depression
350 was similar in light experiment and dark control. The % PDOC (relative to starting solution) as
351 a function of exposure time over 28 days of experiment ranged from 0 to 5% in peatbog
352 depression and 0 to 10% in thermokarst lake and permafrost spring (**Fig 3 B**).

353 The $SUVA_{254\text{ nm}}$ in photodegradation experiments decreased much stronger than the
354 DOC. The SUVA decrease relative to control was mostly pronounced in permafrost stream
355 (**Fig. 4**). The optical properties of DOC demonstrated sizeable decrease of E_{365}/E_{470} ratio
356 corresponding to UV/vis absorbing functional groups (**Fig. S4 A**), which was consistent with
357 decreasing $SUVA_{254\text{ nm}}$ during sunlight exposure. The E_{254}/E_{436} ratio, corresponding to



358 autochthonous vs. terrestrial DOM, did not demonstrate any sizeable change over the course of
359 experiment (**Fig. S4 B**).

360 Most of major and trace elements did not show any significant (at $p < 0.05$) change in
361 concentration over the photodegradation experiments. Only a few nutrients (P, Fe, Zn, B) and
362 trace metals (Zn, Ti, V, Zr, Nb and Th) demonstrated a decrease in concentration. The decrease
363 of Fe was mostly pronounced in permafrost stream, and did not occur in permafrost depression
364 (**Fig. 5 A**) whereas total dissolved phosphorus systematically decreased, by 20 to 50%, over 28
365 days of sunlight exposure in permafrost depression, thermokarst lake and permafrost stream
366 (**Fig. 5 B**). A decrease of Ti, Zn, Nb and Th also occurred in thermokarst lake and permafrost
367 stream (not shown). Overall, the magnitude of decrease of P, Fe, Ti, V and Zn in
368 photodegradation experiments followed the order “permafrost stream > thermokarst lake >
369 permafrost depression”.

370

371

372 **4. Discussion**

373 *4.1. High stability of dissolved organic matter to bio degradation in surface waters from*
374 *frozen peatland*

375 The unexpected result of this study was very low BDOC fraction, measured not only in
376 large river (Pechora) but also in small stream, thermokarst lake and peatland depressions formed
377 due to permafrost subsidence. According to compilation of available biodegradation studies,
378 the BDOC fraction (28 days) ranges from 3 to 18% (mean 13%) in waters of continuous
379 permafrost zone and from 5 to 15% (mean 14%) in discontinuous permafrost zone (Vonk et al.,
380 2015). This is higher than the 0 to 10 % of BDOC measured for all water objects from the
381 discontinuous permafrost zone in this study. Note that very few biodegradability studies in
382 aquatic systems dealt with frozen peatlands, and all previous incubation experiments used water



383 from mountainous regions on mineral soils and rocks in Scandinavia, Alaskan slope and
384 Canada, yedoma regions of Eastern Siberia, or the Yenisey basin. Only one former
385 biodegradation study in peat mire context demonstrated sizable bioavailability of soil aquatic
386 leachate to lake water bacteria (Roehm et al., 2009), but this work did not deal with pure aquatic
387 endmember, unlike this study. Instead, the BDOC of frozen peatlands surface waters measured
388 for the Bolshezemelskaya Tundra inland waters was comparable with the value suggested by
389 Vonk et al (2015) for non-permafrost aquatic DOC (0-1 %).

390 Another important point revealed in previous work on biodegradation of Arctic waters
391 is that aquatic BDOC in large streams and rivers decreased as the Arctic summer progressed
392 (Vonk et al., 2015), although this pattern was absent for soils and small streams. In our case,
393 thermokarst lake Isino and r. Pechora can be considered as sufficiently large hydrological
394 systems. The sampling was performed in the end of July which is already summer baseflow
395 period and as such 0 to 5 % biodegradable DOC measured for Isino and Pechora in this study
396 is comparable with 0 to 20% BDOC loss reported in large streams and rivers at ~200 Julian day
397 (Vonk et al., 2015). However, small stream and permafrost subsidence remain clearly at the
398 very low edge of BDOC % lost reported for soils and streams in summer. In the estuarine zone
399 of largest European Arctic permafrost-free river, Severnaya Dvina, there was no measurable
400 biodegradation in spring, when the DOM was dominated by allochthonous sources, but a 15 to
401 20% decrease of DOC occurred during first 300 h in river water collected in August, when
402 sizeable phytoplankton productivity was observed (Shirokova et al., 2017b). In laboratory
403 experiments with individual cultures, moss and peat leachates were also sizably biodegraded
404 over 1-2 days of exposure (Shirokova et al., 2017a), whereas the same bacterial species were
405 not capable degrading DOM from surface waters draining peatland and moss covered bogs
406 (Oleinikova et al., 2018). This is consisted with a priming effect, a possible mechanism by
407 which inputs of biolabile DOC from plant litter enhance the bioavailability of stable DOC



408 components in aquatic systems, resulting in higher rates of microbial remineralization (Textor
409 et al., 2018).

410 Mechanistic reasons for extremely low bioavailability of DOC from studied peatlands
411 remain unclear and require in-depth analysis of DOM molecular structure and stoichiometry as
412 well as high resolution microbial approaches. It is known that the DOM released from frozen
413 soils contains high proportions of biologically labile protein-like and photochemically reactive
414 aromatic substances (Gao et al., 2018). Following the pioneering study of Ward et al. (2017),
415 we hypothesize that, similar to DOC from organic (non-permafrost) layer, the concentration of
416 high-lability, aliphatic-like DOC in surface waters of frozen peatlands is too low to sustain
417 microbial population, or that this aquatic DOC, remaining after microbial processing of soil
418 porewater DOC is of low lability for microbes capable to degrade aliphatic-like DOC and
419 inhabiting aerobic zone of permafrost surface waters. The constant pattern of UV_{254} absorbency
420 in biodegradation experiment was consistent with negligible change in BDOC over 28 days of
421 incubation. In comparison, the biodegradation of peat water from European boreal zone was
422 associated with an increase in SUVA by up to 7.4 %, which also implies an increase in the
423 proportion of aromatic compounds (Hulatt et al., 2014). The total bacterial number in studied
424 surface waters $(0.5-5) \times 10^6$ cell mL⁻¹ is in excellent agreement with other studies of thermokarst
425 peatland lake waters (Deshpande et al., 2016). Following these researchers, we suggest that the
426 reason of low biodegradability of peatland humic waters is that the majority of active bacteria
427 are associated with particles ($> 3 \mu\text{m}$) rather than present as free-living cells ($< 1 \mu\text{m}$) capable
428 to DOC processing. However, further mechanistic studies of model aquatic bacterial
429 communities capable to affect the degradation of DOM from different terrestrial sources are
430 necessary (Logue et al., 2016).

431 Interestingly, there was no measurable difference in BDOC at 4, 23 and 37°C, as the
432 proportion of BDOC at all temperatures for each system was below 5%. This result allows



433 preliminary prediction of possible consequence of climate change and surface water heating in
434 high latitudes. In a short-term climate warmings scenario, or assuming fast heating of surface
435 waters due to prolonged heat wave of draught occurring both in European, permafrost-free (see
436 Shirokova et al., 2013a) and western Siberian (Pokrovsky et al., 2013) permafrost-bearing
437 peatlands, we do not foresee any measurable change in biodegradability of DOM from the water
438 column. Under even most extreme heating scenario of thermokarst lakes, river and depressions
439 of the frozen peatland territories, the short-term bio-processing of aquatic DOM may remain
440 close to zero.

441

442 *4.2. Negligible impact of photodegradation on DOM transformation in inland waters of*
443 *frozen peatlands*

444 The second main result of this work was high stability of surface waters DOM to
445 sunlight exposure. Over 28 d of incubation in outdoor pools at the conditions corresponding to
446 surface (< 0.05 m depth) water layer of thermokarst lakes and streams from permafrost zone,
447 the change in DOC concentration was less than **5-10%** of the initial value and was not
448 distinguishable from that in the dark control (**Fig. 3 A, B**). Therefore, the DOM of all frozen
449 peatland is quite refractory and not subject to measurable photodegradation over 4 weeks of
450 exposure. This time is comparable with the water residence time in small depressions of the
451 frozen peatland (Novikov et al., 2009) and small thermokarst thaw ponds of frozen palsa
452 peatbog (Manasygov et al., 2015) but much higher than the water travel time in small streams
453 (< 10 km long) and in the lower reaches of Pechora river, from the site of sampling till the
454 Arctic Ocean (ca. several days). This result apparently contradicts the recent paradigm that the
455 photochemical oxidation may account for 70 to 95% of total DOC processed in the water
456 column of arctic lakes, rivers and soils (Cory et al., 2013, 2014; Ward and Cory, 2016; Ward et
457 al., 2017). However, the conclusion of this group of authors is based on study of distilled water



458 leachates of mineral soils, headwater streams, fresh permafrost thaw sites and lakes of N.
459 Alaska slopes, developed on mineral substrates. In contrast, the results of DOM photolysis in
460 polygonal and runnel ponds located in frozen peatlands (2 m peat, 40-60 cm ALT) of continuous
461 permafrost regions of Canada High Arctic demonstrated a relatively fast decay of color and
462 fluorescence, but insignificant losses of DOC over 12 days of exposure time (Laurion and
463 Mladenov, 2013). Recently, no measurable photochemical loss of ancient permafrost DOC has
464 been revealed in the thawing yedoma permafrost sites of the Kolyma River, its tributaries and
465 streams (Stubbins et al., 2017). Another recent study of DOM photodegradation in boreal high-
466 latitude peatland streams of the White Sea watershed demonstrated only 10% decrease in DOC
467 concentration over 10 days of incubation under sunlight (Oleinikova et al., 2017). In the
468 estuarine zone of the largest European Arctic river draining wetland- and forest-dominated
469 permafrost-free territory (Severnaya Dvina), we did not find any measurable photo-
470 degradation of DOM over 1 month of exposure (Chupakova et al., 2018). This comparison
471 clearly demonstrate highly contrasting DOM photolability between the aquatic systems of N.
472 America, draining through mineral soil substrates, and that of boreal and subarctic peatlands.

473 Further, due to high homogeneity of organic substrate surrounding studied waters and
474 similar allochthonous origin of DOM in all surface waters of frozen peatlands, there is no
475 dramatic difference in DOM photodegradability over the hydrological continuum in NE
476 European Arctic, which also contrasts the results obtained in aquatic systems on mineral soils
477 (Cory et al., 2007, 2013; Reader et al., 2014). It is possible that either 1) photochemical
478 degradation of humic peat waters occurs very fast, during first ours to days upon their exposure
479 to sunlight or 2) that the nature of DOM is so refractory that much longer exposure periods, on
480 the order of several months to years (as in the Arctic coast) are necessary to photodegrade the
481 DOM from frozen peatlands. The first explanation is consistent with recent experiments on
482 photodegradation of fresh peat mire water, collected in taiga region of NW Russia, where about



483 50% of bogwater DOC was photodegraded over 2 days of exposure to sunlight (Oleinikova et
484 al., 2017).

485 As such, it is possible that all surface waters sampled for experiments in this study,
486 including stagnant water in permafrost depression, were already contacting with sunlight for
487 more than several days and thus became photo-resistant. Assuming the maximal possible DOC
488 loss due to photolysis assessed in our experiments ($0.1 \text{ mg C L}^{-1} \text{ d}^{-1}$ corresponding to a loss of
489 3 mg/L during 28 days) and the light penetration depth of 0.5 m which is comparable with the
490 typical depth of studied water bodies, the photodegradation can supply less than 10 % of total
491 CO_2 emission flux from the water surfaces of frozen peatlands ($0.4\text{-}0.8 \text{ g C m}^{-2} \text{ d}^{-1}$ in this work;
492 0.8 to $4.4 \text{ C m}^{-2} \text{ d}^{-1}$ in western Siberian rivers and streams, located on very similar context of
493 frozen peat bogs, Serikova et al., 2018). The maximal PDOC value measured in this work is
494 also at the lower end range of DOM photodegradation contribution to C flux in North European
495 boreal and subarctic settings. Thus, DIC annual photo-production contributed between 1 to 8
496 % of CO_2 emissions from a humic lake in south of Sweden (Groeneveld et al., 2016) and
497 globally in the boreal and subarctic zone, sunlight-induced CO_2 emissions represent about one
498 tenth to the CO_2 emission from lakes and reservoirs (Koehler et al., 2014).

499 The evolutions of optical properties of DOM as a function of exposure time in different
500 samples were consistent with the mechanisms of photo-sensitive DOM removal during
501 irradiation. The ratio E_{365}/E_{470} is known to correlate with the degree of condensation of DOM
502 aromatic groups and with the degree of humification (Chin et al., 1994; Hur et al., 2006)
503 whereas UV_{254} is used as proxy for aromatic C and source of DOM (Chen et al., 1977; Uyguner
504 and Bekbolet, 2005). The optical properties of DOC were much less conservative under sunlight
505 exposure compared to total dissolved C concentration, as $\text{UV}_{254 \text{ nm}}$ and E_{365}/E_{470} ratio sizably
506 decreased in the course of experiments. Numerous studies of allochthonous riverine DOM also
507 revealed that photodegradation of colored DOM (CDOM) and SUVA_{254} were much greater



508 than DOC losses (Spencer et al., 2009; Reche et al., 2000; Vähätalo and Wetzel, 2004; Mostofa
509 et al., 2011; Bittar et al., 2015; Gareis and Lesack, 2018). A decrease of E_{365}/E_{470} corresponded
510 to removal of UV rather than visual light absorbing functional groups, whereas a constant
511 pattern of E_{254}/E_{436} ratio in the hydrological continuum ‘depression → stream → lake → river’
512 was consistent with lack of autochthonous DOM in all studied water objects, which were
513 dominated by terrestrial (aromatic) DOM from peat horizons. Overall, our observations confirm
514 the conclusion achieved from a recent compilation of available data across the world that
515 degradation processes act preferentially on CDOM rather than DOC concentration (Massicotte
516 et al., 2017; Oleinikova et al., 2017).

517 In contrast to DOC, sizeable removal of dissolved P and Fe together with some related
518 trace elements (Ti, V, Zn, Nb) during photolysis of surface waters reflects transformation and
519 coagulation of Fe-rich colloids, that behave independent on organic colloids in humic waters
520 (Vasyukova et al., 2010; Pokrovsky et al., 2016). This precipitation of Fe hydroxides together
521 with P and insoluble trace elements was mostly pronounced in permafrost stream which had
522 the highest pH and thus allowed minimal stability of Fe(III) hydroxides that were coagulated
523 after removal of small amount of DOM that stabilized colloidal Fe (Oleinikova et al., 2017).

524

525 *4.3. Lack of bio- and photodegradation in humic surface waters of frozen peat bogs*
526 *despite sizeable CO₂ emission*

527 The main fundamental result of the present study is that, despite well-known
528 supersaturation of lentic and lotic waters of frozen peatlands to atmospheric pCO₂, the surface
529 waters of frozen peatlands exhibit negligible bio- and photo-degradability over time scale (28
530 days) comparable with water residence time in various reservoirs. This is at odds with the
531 dominant paradigm that bio- and photodegradation control the DOC removal from arctic
532 aquatic ecosystems (Abbot et al., 2014; Cory et al., 2014; Spencer et al., 2015). Given



533 incontestable bio- and photodegradability of peat pore waters and frozen soil extracts reported
534 across the Arctic (Vonk et al., 2015; Selvam et al., 2017), this strongly suggests that the DOM
535 that arrives to small rivers and even permafrost depressions from the soils via lateral soil outflux
536 is already highly degraded. This is consistent with general idea that rates of DOM
537 photochemical alteration and rates of microbial responses to altered DOM are typically rapid,
538 from minutes to days (Cory and Kling, 2018). As such, the majority of elevated CO₂ measured
539 in surface waters of permafrost peat landscape originates from degradation of DOM in soil
540 water, not in surface water. We believe that the degradation of soil fluids occurs very fast and
541 completes within first hours or days. This is shorter than the residence time of water in
542 permafrost depressions, thaw ponds and rivers. As a result, we did not detect sizeable bio- and
543 photodegradation of residual DOM in various types of inland waters from permafrost
544 landscapes. In order to explain persistent CO₂ supersaturation of inland waters from peatlands,
545 we suggest that benthic respiration of stream, lake and river sediments produce sizeable amount
546 of CO₂ thus increasing overall C emission potential of the aquatic systems (MacIntyre et al.,
547 2018; Valle et al., 2018). For example, anaerobic C mineralization of thermokarst lake
548 sediments is fairly well established in discontinuous permafrost zone of peat bogs in western
549 Siberia (Audry et al., 2011) and Canada (Deshpande et al., 2017).

550 The findings of this study and widely reported dominance of non-biodegradable DOC
551 (0-1% BDOC) in large rivers and streams of the non-permafrost zone (Vonk et al., 2015)
552 suggest that 1) the majority of BDOC is degraded before its arrival to large aquatic reservoirs,
553 and 2) the CO₂ supersaturation and emission of surface waters from frozen peatlands is due to
554 soil pore water and sediment respiration rather than aerobic bio- and photo-degradation of DOM
555 in the water column. Further, the non-increase in BDOC fraction during temperature rise from
556 4 to 37°C implies that, within the climate warming scenario, the heating of peat surface waters
557 will be a minor factor of overall CO₂ balance. Instead, the change of water path and residence



558 time in pore waters of frozen peatlands, the rate of supra-permafrost water delivery, and
559 magnitude of benthic respiration in large rivers and thermokarst lakes may control the CO₂
560 emission from inland waters.

561

562 **Conclusions**

563 This work revealed high resistance of surface waters collected in permafrost peatland to
564 both bio- and photo-degradation. Less than 5-10% of the initial aquatic DOC was removed over
565 1 month of dark aerobic incubation at 4, 22 and 37°C as well as during sunlight exposure of
566 sterile-filtered waters. In contrast to expected differences in bio- and photo-lability between
567 small permafrost subsidences, streams, large lake and the Pechora River, there was no
568 measurable difference in surface waters BDOC concentration along the hydrological
569 continuum. The contribution of aerobic DOM biodegradation within the water column to
570 observed CO₂ supersaturations and net CO₂ emission fluxes from bog water, lakes, streams and
571 rivers of peatland territories located within discontinuous permafrost zone is less than 10%.
572 Despite decrease in CDOM during photolysis, this process does not significantly contribute to
573 total DOC degradation and C emission from the surface of inland waters of frozen peatlands.

574 We hypothesize that refractory nature of DOM from frozen peatlands which is already
575 processed in soil waters before arriving to lentic and lotic surface reservoirs create unfavorable
576 conditions for biodegradation. The reason for high stability of DOM from frozen peatland to
577 photolysis is less clear but can be linked to fast photo-degradation of peat bog and soil shallow
578 underground) waters after their exposure to the surface, occurring within the first hours to days.
579 We conclude on negligible impact of bio- and photo-degradation on DOM processing and CO₂
580 emission in surface waters of frozen peatlands. This calls for future work to quantify bio- and
581 photo-lability of peat pore waters, thawing soil ice, and suprapermafrost flow, which deliver
582 the DOM to the rivers, lakes and depressions.



583 Acknowledgements

584 This work was supported by RFFI (RFBR) grants No 17-05-00348_a and 17-05-
585 00342_a, Program FANO No 0409-2015-0140, RFFI No 18-05-01041 and UroRAN No 18-9-
586 5-29. Additional funding from JPI Climate initiative, financially supported by VR (the Swedish
587 Research Council) grant no. 325-2014-6898, is also acknowledged.

588

589 References

- 590 Abbott, B. W., Larouche, J. R., Jones, J. B., Bowden, W. B., and Balser, A. W.: Elevated
591 dissolved organic carbon biodegradability from thawing and collapsing permafrost, *J.*
592 *Geophys. Res.*, 119, 2049–2063, 2014.
- 593 Amado, A. M., Cotner, J. B., Cory, R. M., Edhlund, B. L., and McNeill, K.: Disentangling the
594 interactions between photochemical and bacterial degradation of dissolved organic matter:
595 amino acids play a central role, *Microb. Ecol.*, 69(3), 554–566, 2014.
- 596 Andersson, M. G. I., Catalán, N., Rahman, Z., Tranvik, L. J., and Lindström, E. S.: Effects of
597 sterilization on dissolved organic carbon (DOC) composition and bacterial utilization of
598 DOC from lakes, *Aquat. Microb. Ecol.*, 82, 199–208, 2018.
- 599 Ask, J., Karlsson, J., and Jansson, M.: Net ecosystem production in clear-water and brown-
600 water lakes, *Glob. Biogeochem. Cycles*, 26, GB1017, doi:10.1029/2010GB003951, 2012.
- 601 Audry, S., Pokrovsky, O. S., Shirokova, L. S., Kirpotin, S. N., and Dupré, B.: Organic matter
602 mineralization and trace element post-depositional redistribution in Western Siberia
603 thermokarst lake sediments, *Biogeosciences*, 8, 3341–3358, 2011.
- 604 Berggren, M., Laudon, H., Haei, M., Ström, L., and Jansson, M.: Efficient aquatic bacterial
605 metabolism of dissolved low-molecular-weight compounds from terrestrial sources, *ISME*
606 *J.*, 4, 408–416, 2010.
- 607 Bittar, T. B., Vieira, A. A. H., Stubbins, A., and Mopper, K.: Competition between
608 photochemical and biological degradation of dissolved organic matter from the
609 cyanobacteria *Microcystis aeruginosa*, *Limnol. Oceanogr.*, 60, 1172–1194, 2015.
- 610 Brittain, J. F., Gislason, G. M., Ponomarev, V. I., Bogen, J., Jensen, A. J., Khokhlova, L. G.,
611 Kochanov, S. K., Kokovkin, A. V., Melvold, K., Olafsson, J. S., Pettersson, L.-E., and
612 Stenina, A. S.: Arctic Rivers (chapter 9), pp. 337–379. In: *Rivers of Europe*, Eds: Tockner
613 K., Uehlinger U., Robinson C.T., Academic Press Elsevier, 2009.
- 614 Chen, Y., Senesi, N., and Schnitzer, M.: Information provided on humic substances by E4/E6
615 ratios, *Soil Sci. Soc. Amer. J.*, 41, 352–358, 1977.
- 616 Chin, Y.-P., Aiken, G., and O’Loughlin, E.: Molecular weight, polydispersity, and
617 spectroscopic properties of aquatic humic substances. *Environ. Sci. Technol.*, 28, 1853-
618 1858, 1994.
- 619 Chupakova, A. A., Chupakov, A. V., Neverova, N. V., Shirokova, L. S., and Pokrovsky, O. S.:
620 Photodegradation of river dissolved organic matter and trace metals in the largest European
621 Arctic estuary. *Sci. Total Environ.*, 622–623, 1343–1352, 2018.
- 622 Cole, J. J. and Caraco, N.: Atmospheric exchange of carbon dioxide in a low-wind oligotrophic
623 lake measured by the addition of SF₆. *Limnol. Oceanogr.*, 43, 647–656, 1998.
- 624 Cory, R. M., McKnight, D., Chin, Y. P., Miller, P., and Jaros, C. L.: Chemical characteristics
625 of fulvic acids from Arctic surface waters: Microbial contributions and photochemical
626 transformations, *J. Geophys. Res.*, 112, G04S51, doi:10.1029/2006JG000343, 2007.



- 627 Cory, R. M., Crump, B. C., Dobkowski, J. A., and Kling, G. W.: Surface exposure to sunlight
628 stimulates CO₂ release from permafrost soil carbon in the Arctic, *Proc. Natl. Acad. Sci.*
629 USA, 110(9), 3429-3434, 2013.
- 630 Cory, R. M., Ward, C. P., Crump, B. C., and Kling, G. W.: Sunlight controls water column
631 processing of carbon in arctic fresh waters, *Science*, 345, 925-928, 2014.
- 632 Cory, R. M., Harrold, K. H., Neilson, B. T., Kling, G. W.: Controls on dissolved organic matter
633 (DOM) degradation in a headwater stream: the influence of photochemical and
634 hydrological conditions in determining light-limitation or substrate-limitation of photo-
635 degradation, *Biogeosciences*, 12, 6669–6685, 2015.
- 636 Cory, R. M., Kling, G. W.: Interactions between sunlight and microorganisms influence
637 dissolved organic matter degradation along the aquatic continuum, *Limnol. Oceanogr.*
638 Lett., 3, 102–116, 2018.
- 639 Deshpande, B. N., Maps, F., Matveev, A., and Vincent, W. F., 2017. Oxygen depletion in
640 subarctic peatland thaw lakes, *Arctic Science*, 3(2), 406-428, 2017.
- 641 Deshpande, B. N., Crevecoeur, S., Matveev, A., and Vincent, W. F.: Bacterial production in
642 subarctic peatland lakes enriched by thawing permafrost, *Biogeosciences*, 13, 4411-4427,
643 2016.
- 644 Gao, L., Zhou, Z., Reyes, A. V., and Guo, L.: Yields and characterization of dissolved organic
645 matter from different aged soils in northern Alaska, *J. Geophys. Res.: Biogeosciences*, 123,
646 2035–2052, 2018.
- 647 Gareis, J. A. L., and Lesack, L. F. W.: Photodegraded dissolved organic matter from peak
648 freshet river discharge as a substrate for bacterial production in a lake-rich great Arctic
649 delta, *Arctic Science*, 4(4), 557-583, 2018.
- 650 Groeneveld, M., Tranvik, L., Natchimuthu, S., and Koehler, B.: Photochemical mineralisation
651 in a boreal brown water lake: considerable temporal variability and minor contribution to
652 carbon dioxide production, *Biogeoscience*, 13, 3931-3943, 2016.
- 653 Helms, J. R., Stubbins, A., Ritchie, J. D., Minor, E. C., Kieber, D. J., Mopper, K.: Absorption
654 spectral slopes and slope ratios as indicators of molecular weight, source, and
655 photobleaching of chromophoric dissolved organic matter, *Limnol. Oceanogr.*, 53(3), 955-
656 969, 2008.
- 657 Holmes, R. M., McClelland, J. W., Raymond, P. A., Frazer, B. B., Peterson, B. J., and Stieglitz,
658 M.: Lability of DOC transported by Alaskan rivers to the Arctic Ocean, *Geophys. Res. Lett.*,
659 35, L03402, doi:10.1029/2007GL032837, 2008.
- 660 Hulatt, C. J., Kaartokallio, H., Asmala, E., Autio, R., Stedmon, C. A., Sonninen, E., Oinonen,
661 M., and Thomas, D. N.: Bioavailability and radiocarbon age of fluvial dissolved organic
662 matter (DOM) from a northern peatland-dominated catchment: effect of land-use change,
663 *Aquat. Sci.*, 76(3), 393-404, 2014.
- 664 Hur, J., Williams, M. A., and Schlautman, M. A.: Evaluating spectroscopic and chromatographic
665 techniques to resolve dissolved organic matter via end member mixing analysis,
666 *Chemosphere*, 63, 387-402, 2006.
- 667 Ilina, S. M., Drozdova, O. Yu., Lapitsky, S. A., Alekhin, Yu. V., Demin, V. V., Zavgorodnaya,
668 Yu. A., Shirokova, L. S., Viers, J., and Pokrovsky, O. S.: Size fractionation and optical
669 properties of dissolved organic matter in the continuum soil solution-bog-river and terminal
670 lake of a boreal watershed, *Org. Geochem.*, 66, 14–24, 2014.
- 671 Kaiser, K., Canedo-Oropeza, M., McMahon, R., and Amon, R. M. W.: Origins and
672 transformations of dissolved organic matter in large Arctic rivers, *Sci. Reports*, 7, 13064,
673 2017.



- 674 Karlsson, J., Jansson, M., and Jonsson, A.: Respiration of allochthonous organic carbon in
675 unproductive forest lakes determined by the Keeling plot method, *Limnol. Oceanogr.*, 52,
676 603–608, 2007.
- 677 Koehler, B., Landelius, T., Weyhenmeyer, G. A., Machida, N., and Tranvik, L.J.: Sunlight-
678 induced carbon dioxide emissions from inland waters, *Global Biogeochem. Cycles*, 28,
679 696–711, 2014.
- 680 Köhler, S., Buffam, I., Jonsson, A., and Bishop, K.: Photochemical and microbial processing
681 of stream and soil water dissolved organic matter in a boreal forested catchment in northern
682 Sweden, *Aquat. Sci.*, 64, 269–281, 2002.
- 683 Lapiere, J.-F., Guillemette, F., Berggren, M., and del Giorgio, P. A.: Increases in terrestrially
684 derived carbon stimulate organic carbon processing and CO₂ emissions in boreal aquatic
685 ecosystems, *Nature Comm.*, 4, 2972, doi:10.1038/ncomms3972, 2013.
- 686 Larouche, J. R., Abbott, B. W., Bowden, W. B., Jones, and J. B.: The role of watershed
687 characteristics, permafrost thaw, and wildfire on dissolved organic carbon biodegradability
688 and water chemistry in Arctic headwater streams, *Biogeosciences*, 12, 4221–4233, 2015.
- 689 Laurion, I., and Mladenov, N.: Dissolved organic matter photolysis in Canadian Arctic thaw
690 ponds, *Environ. Res. Lett.*, 8, 035026, doi.org/10.1088/1748-9326/8/3/035026, 2013.
- 691 Logue, J. B., Stedmon, C. A., Kellerman, A. M., Nielsen, N. J., Andersson, A. F., Laudon, H.,
692 Lindström, E. S., and Kritzberg, E. S.: Experimental insights into the importance of aquatic
693 bacterial community composition to the degradation of dissolved organic matter, *ISME J.*,
694 10, 533–545, 2016.
- 695 Lou, T., and Xie, H.: Photochemical alteration of the molecular weight of dissolved organic
696 matter, *Chemosphere*, 65, 2333–2342, 2006.
- 697 MacIntyre, S., Cortes, A., and Sadro, S.: Sediment respiration drives circulation and production
698 of CO₂ in ice-covered Alaskan arctic lakes, *Limnol. Oceanogr. Lett.*, 3, 302–310, 2018.
- 699 Manasyov, R. M., Pokrovsky, O. S., Kirpotin, S. N., Shirokova, L. S.: Thermokarst lake waters
700 across permafrost zones of Western Siberia, *Cryosphere* 8, 1177–1193, 2014.
- 701 Manasyov, R. M., Vorobyev, S. N., Loiko, S. V., Kritzkov, I. V., Shirokova, L. S.,
702 Shevchenko, V. P., Kirpotin, S. N., Kulizhsky, S. P., Kolesnichenko, L. G., Zemtzov, V.
703 A., Sinkin, V. V., and Pokrovsky, O. S.: Seasonal dynamics of organic carbon and metals
704 in thermokarst lakes from the discontinuous permafrost zone of western Siberia,
705 *Biogeosciences*, 12, 3009–3028, 2015.
- 706 Mann, P. J., Davydova, A., Zimov, N., Spencer, R. G. M., Davydov, S., Bulygina, E., Zimov,
707 S., Holmes, R. M.: Controls on the composition and lability of dissolved organic matter in
708 Siberia's Kolyma River basin, *J. Geophys. Res.*, 117, G01028, doi:
709 10.1029/2011JG001798, 2012.
- 710 Mann, P. J., Sobczak, W. V., LaRue, M. M., Bulygina, E., Davydova, A., Vonk, J. E., Schade,
711 J., Davydov, S., Zimov, N., Holmes, R. M., Spencer, R. G. M.: Evidence for key enzymatic
712 controls on metabolism of Arctic river organic matter, *Global Change Biol.*, 20(4), 1089–
713 1100, 2014.
- 714 Mann, P. J., Eglinton, T. I., Mcintyre, C. P., Zimov, N., Davydova, A., Vonk, J. E., Holmes, R.
715 M., Spencer, R. G. M.: Utilization of ancient permafrost carbon in headwaters of Arctic
716 fluvial networks, *Nat. Commun.*, 6, doi: 10.1038/ncomms8856, 2015.
- 717 Massicotte, P., Asmala, E., Stedmon, C., Markager, S.: Global distribution of dissolved matter
718 along the aquatic continuum: Across rivers, lakes and oceans, *Sci. Total Environ.*, 609,
719 180–191, 2017.
- 720 McCallister, S. L., and del Giorgio, P. A.: Direct measurement of the $\delta^{13}\text{C}$ signature of carbon
721 respired by bacteria in lakes: Linkages to potential carbon sources, ecosystem baseline
722 metabolism, and CO₂ fluxes, *Limnol. Oceanogr.*, 53(4), 1204–1216, 2008.



- 723 Moran, M. A., Sheldon, W. M., and Zepp, R. G.: Carbon loss and optical property changes
724 during long-term photochemical and biological degradation of estuarine dissolved organic
725 matter, *Limnol. Oceanogr.*, 45, 1254–1264, 2000.
- 726 Mostofa, K. M. G., Yoshioka, T., Konohira, E., and Tanoue, E.: Photodegradation of
727 fluorescent dissolved organic matter in river waters, *Geochem. J.*, 41, 323–331, 2007.
- 728 Mostofa, K. M. G., Wu, F., Liu, C-Q., Vione, D., Yoshioka, T., Sakugawa, H., and Tanoue, E.:
729 Photochemical, microbial and metal complexation behavior of fluorescent dissolved
730 organic matter in the aquatic environments, *Geochem. J.*, 45, 235–254, 2011.
- 731 Novikov, S. M., Moskvina, Y. P., Trofimov, S. A., Usova, L. I., Batuev, V. I., Tumanovskaya, S.
732 M., Smirnova, V. P., Markov, M. L., Korotkevich, A. E., and Potapova, T. M.: Hydrology
733 of bog territories of the permafrost zone of western Siberia, *BBM publ. House, St.*
734 *Petersbourg*, 535 pp. (in Russian), 2009.
- 735 Oleinikova, O., Drozdova, O. Y., Lapitskiy, S. A., Bychkov, A. Y., and Pokrovsky, O. S.:
736 Dissolved organic matter degradation by sunlight coagulates organo-mineral colloids and
737 produces low-molecular weight fraction of metals in boreal humic waters, *Geochim.*
738 *Cosmochim. Acta*, 211, 97–114, 2017.
- 739 Oleinikova, O., Shirokova, L. S., Drozdova, O. Y., Lapitskiy, S. A., and Pokrovsky, O. S.: Low
740 biodegradability of dissolved organic matter and trace metal from subarctic waters by
741 culturable heterotrophic bacteria, *Sci. Total Environ.*, 618, 174–187, 2018.
- 742 Pokrovsky, O. S., Shirokova, L. S., Zabelina, S. A., Vorobieva, T. Ya., Moreva, O. Yu., Klimov,
743 S. I., Chupakov, A. V., Shorina, N. V., Kokryatskaya, N. M., Audry, S., Viers, J., Zoutien,
744 C., and Freydier, R.: Size fractionation of trace elements in a seasonally stratified boreal
745 lakes: Control of organic matter and iron colloids, *Aquat. Geochem.*, 18, 115–139, 2012.
- 746 Pokrovsky, O. S., Shirokova, L. S., Kirpotin, S. N., Kulizhsky, S. P., Vorobiev, S. N.: Impact
747 of Western Siberia heat wave 2012 on greenhouse gases and trace metal concentration in
748 thaw lakes of discontinuous permafrost zone, *Biogeosciences*, 10, 5349–5365, 2013.
- 749 Pokrovsky, O. S., Manasyrov, R. M., Shirokova, L. S., Loiko, S. V., Krickov, I. V., Kopysov,
750 S., and Kirpotin, S. N.: Permafrost coverage, watershed area and season control of
751 dissolved carbon and major elements in western Siberia rivers, *Biogeosciences*, 12, 6301–
752 6320, 2015.
- 753 Pokrovsky, O. S., Manasyrov, R. M., Loiko, S. V., and Shirokova, L. S.: Organic and organo-
754 mineral colloids of discontinuous permafrost zone, *Geochim. Cosmochim. Acta*, 188, 1–
755 20, 2016.
- 756 Porcal, P., Dillon, P. J., and Molot, L. A.: Photochemical production and decomposition of
757 particulate organic carbon in a freshwater stream, *Aquat. Sci.*, 75, 469–482, 2013.
- 758 Porcal, P., Dillon, P. J., and Molot, L. A.: Interaction of extrinsic chemical factors affecting
759 photodegradation of dissolved organic matter in aquatic ecosystems, *Photochem.*
760 *Photobiol. Sci.*, 13, 799–812, 2014.
- 761 Porcal, P., Dillon, P. J., and Molot, L. A.: Temperature dependence of photodegradation of
762 dissolved organic matter to dissolved inorganic carbon and particulate organic carbon, *Plos*
763 *ONE*, 10(6), e0128884, DOI:10.1371/journal.pone.0128884, 2015.
- 764 Porter, K. G., and Feig, Y. S.: The use of DAPI for identifying and counting aquatic microflora,
765 *Limnol. Oceanogr.*, 25: 943–948, 1980.
- 766 Reader, H. E., Stedmon, C. A., and Kritzberg, E. S.: Seasonal contribution of terrestrial organic
767 matter and biological oxygen demand to the Baltic Sea from three contrasting river
768 catchments, *Biogeosciences* 11, 3409–3419, 2014.



- 769 Reche, I., Pace, M. L., and Cole, J. J.: Modeled effects of dissolved organic carbon and solar
770 spectra on photobleaching in lake ecosystems, *Ecosystems* 3, 419-432, 2000.
- 771 Roehm, C. L., Giesler, R., Karlsson, J.: Bioavailability of terrestrial organic carbon to lake
772 bacteria: The case of a degrading subarctic permafrost mire complex, *J. Geophys. Res.*,
773 114, G03006, doi: 10.1029/2008JG000863, 2009.
- 774 Selvam, B. P., Lapierre, J.-F., Guillemette, F., Voigt, C., Lamprecht, R. E., Biasi, C.,
775 Christensen, T. R., Martikainen P. J., and Berggren, M.: Degradation potentials of
776 dissolved organic carbon (DOC) from thawed permafrost peat. *Scientific Reports*, 7, Art
777 No 45811, doi: 10.1038/srep45811, 2016.
- 778 Serikova, S., Pokrovsky, O. S., Ala-aho, P., Kazantsev, V., Kirpotin, S. N. Kopysov, S. G.,
779 Krickov, I. V., Laudon, H., Manasyov, R. M., Shirokova, L. S., Sousby, C., Tetzlaff, D.,
780 Karlsson, J.: High riverine CO₂ emissions at the permafrost boundary of Western Siberia.
781 *Nature Geoscience*, 11, 825-829, 2018.
- 782 Shirokova, L. S., Pokrovsky, O. S., Moreva, O. Y., Chupakov, A. V., Zabelina, S. A., Klimov,
783 S. I., Shorina, N. V., Vorobieva T. Y.: Decrease of concentration and colloidal fraction of
784 organic carbon and trace elements in response to the anomalously hot summer 2010 in a
785 humic boreal lake, *Sci. Tot. Environ.*, 463-464, 78–90, 2013a.
- 786 Shirokova, L. S., Pokrovsky, O. S., Kirpotin, S. N., Desmukh, C., Pokrovsky, B. G., Audry, S.,
787 and Viers, J.: Biogeochemistry of organic carbon, CO₂, CH₄, and trace elements in
788 thermokarst water bodies in discontinuous permafrost zones of Western Siberia,
789 *Biogeochemistry*, 113, 573–593, 2013b.
- 790 Shirokova, L. S., Bredoire, R., Rolls, J. L., and Pokrovsky, O. S.: Moss and peat leachate
791 degradability by heterotrophic bacteria: fate of organic carbon and trace metals,
792 *Geomicrobiol. J.*, 34(8), 641-655, 2017a.
- 793 Shirokova, L. S., Chupakova, A. A., Chupakov, A. V., and Pokrovsky, O.S.: Transformation of
794 dissolved organic matter and related trace elements in the mouth zone of the largest
795 European Arctic river: experimental modeling, *Inland Waters*, 7(3), 272-282, 2017b.
- 796 Spencer, R. G. M., Stubbins, A., Hernes, P. J., Baker, A., Mopper, K., Aufdenkampe, A. K.,
797 Dyda, R. Y., Mwamba, V. L., Mangangu, A. M., Wabakghanzi, J. N., Six, J.:
798 Photochemical degradation of dissolved organic matter and dissolved lignin phenols from
799 the Congo River, *J. Geophys. Res.*, 114, G03010, doi: 10.1029/2009JG000968, 2009.
- 800 Spencer, R. G. M., Mann, P. J., Dittmar, T., Eglinton, T. I., McIntyre, C., Holmes, R. M., Zimov,
801 N., Stubbins, A.: Detecting the signature of permafrost thaw in Arctic rivers, *Geophys. Res.*
802 *Let.*, 42, 2830-2835, 2015.
- 803 Stubbins, A., Mann, P. J., Powers, L., Bittar, T. B., Dittmar, T., McIntyre, C. P., Eglinton, T.
804 I., Zimov, N., Spencer, R. G. M.: Low photolability of yedoma permafrost dissolved
805 organic carbon, *J. Geophys. Res. Biogeosci.*, 122, 200-211, doi: 10.1002/2016JG003688,
806 2017.
- 807 Stutter, M. I., Richards, S., and Dawson, J. J. C.: Biodegradability of natural dissolved
808 organic matter collected from a UK moorland stream, *Water Res.*, 47(3), 1169-1180,
809 2013.
- 810 Textor, S. R., Guillemette, F., Zito, P. A., Spencer, R. G. M.: An assessment of dissolved
811 organic carbon biodegradability and priming in blackwater systems, *J. Geophys. Res.*
812 *Biogeosciences*, 123(9), 2998-3015, 2018.
- 813 Uyguner, C., and Bekbolet, M. : Implementation of spectroscopic parameters for practical
814 monitoring of natural organic matter, *Desalination*, 176, 47-55, 2005.
- 815 Valle, J., Gonsior, M., Hairir, M., Enrich-Prast, A., Schmitt-Kopplin, P., Bastviken, D.,
816 Conrad R., and Hertkorn, N.: Extensive processing of sediment pore water dissolved



- 817 organic matter during anoxic incubation as observed by high-field mass spectrometry
818 (FTICR-MS), *Water Research*, 129, 252-263, 2018.
- 819 Vähätalo, A. V., Salonen, K., Münster, U., Järvinen, M., and Wetzel, R. G.: Photochemical
820 transformation of allochthonous organic matter provides bioavailable nutrients in a humic
821 lake, *Acta Hydrobiol.*, 156, 287-314, 2003.
- 822 Vähätalo, A. V. and Wetzel, R.G.: Photochemical and microbial decomposition of
823 chromophoric dissolved organic matter during long (months-years) exposures, *Mar.*
824 *Chem.*, 89, 313-326, 2004.
- 825 Vasyukova, E., Pokrovsky, O. S., Viers, J., Oliva, P., Dupré, B., Martin, F., and Candaudap,
826 F.: Trace elements in organic- and iron-rich surficial fluids of boreal zone: Assessing
827 colloidal forms via dialysis and ultrafiltration, *Geochim. Cosmochim. Acta*, 74, 449-468,
828 2010.
- 829 Vonk, J. E., Tank, S. E., Mann, P. J., Spencer, R. G. M., Treat, C. C., Striegl, R. G., Abbott,
830 B. W., and Wickland K. P.: Biodegradability of dissolved organic carbon in permafrost
831 soils and aquatic systems: a meta-analysis, *Biogeosciences*, 12, 6915-6930, 2015.
- 832 Ward, C. P., Cory, R. M.: Complete and partial photo-oxidation of dissolved organic matter
833 draining permafrost soils, *Environ. Sci. Technol.*, 50(7), 3545-3553, 2016.
- 834 Ward, C. P., Nalven, S. G., Crump, B. C., Kling, G. W., and Cory, R. M.: Photochemical
835 alteration of organic carbon draining permafrost soils shifts microbial metabolic pathways
836 and stimulates respiration, *Nature Comm.*, 8, Art No 772, 2017.
- 837 Wauthy M., Rautio, M., Christoffersen, K. S., Forsstrom, L., Laurion, I., Mariash, H. L.,
838 Peura, S., Vincent, W. F.: Increasing dominance of terrigenous organic matter in
839 circumpolar freshwaters due to permafrost thaw, *Limnol. Oceanogr. Lett.*, 3, 2018, 186–
840 198, 2012.
- 841 Wickland, K. P., Aiken G. R., Butler K., Dornblaser M. M., Spencer R. G. M., and Striegl R.
842 G.: Biodegradability of dissolved organic carbon in the Yukon River and its tributaries:
843 seasonality and importance of inorganic nitrogen. *Glob Biogeochem Cycle* 26,
844 2012gb004342, 2012.
- 845 Wilkinson, G. M., Pace, M. L., Cole, J. J. : Terrestrial dominance of organic matter in north
846 temperate lakes, *Global. Biogeochem. Cycles* 27, 43-51, 2013.
- 847 Winter, A. R., Fish, T. A. E., Playle, R. C., Smith, D. S., and Curtis, P. J.: Photodegradation
848 of natural organic matter from diverse freshwater sources, *Aquat. Toxicol.*, 84, 215-222,
849 2007.

850

851

852

853

854

855

856

857



858

859

860

861

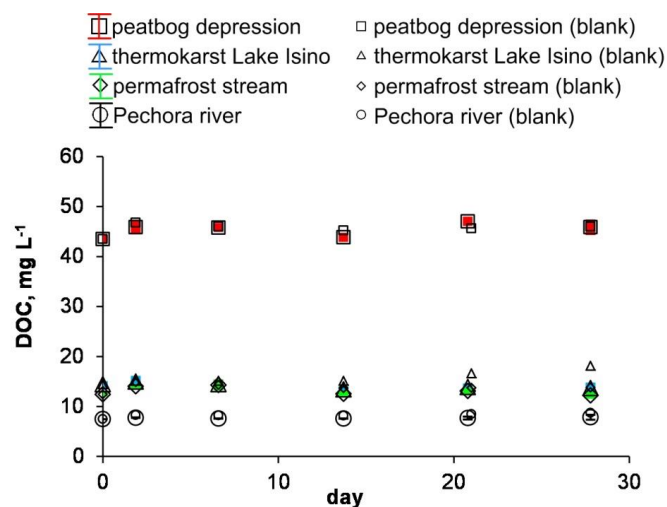
862

863

864

865

866



867

868

869 **Fig. 1.** The DOC concentration over time in biodegradation experiments at 23°C. The
 870 experiments are shown by solid symbols and the control runs are shown by open symbols: red
 871 squares, peatbog depression; green diamonds, permafrost stream; blue triangles, thermokarst
 872 Lake Isino, and black circles, the Pechora River. The error bars represent 1 s.d. of three
 873 replicates and often within the symbol size.

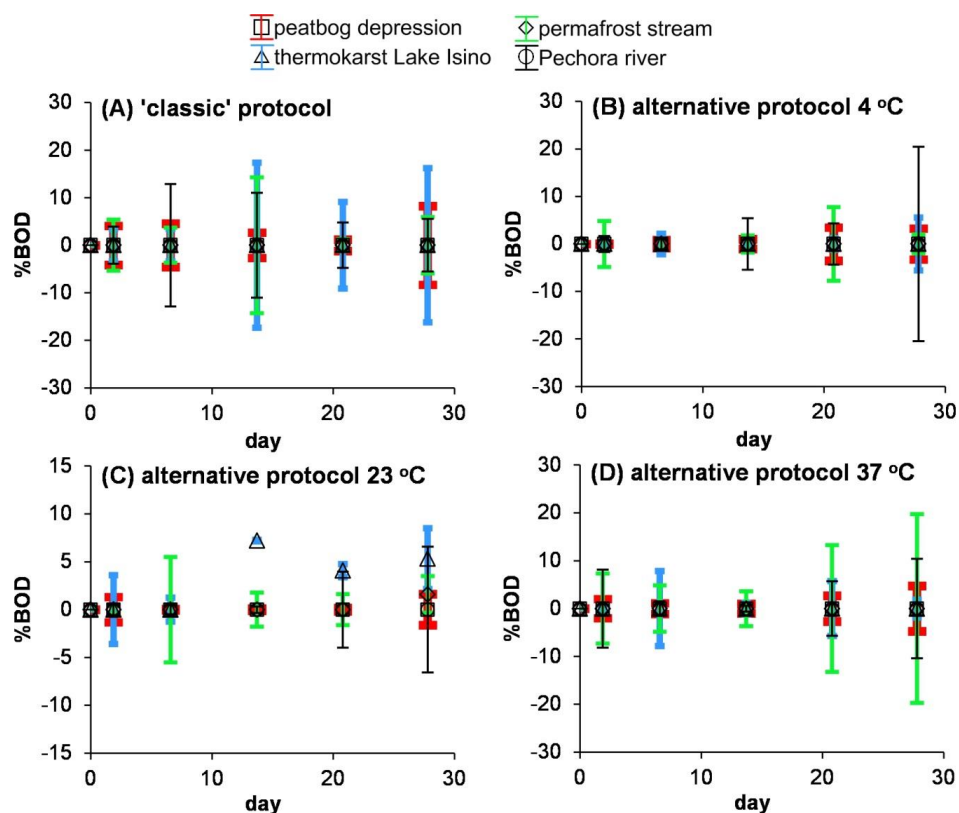
874

875



876

877



878

879

880 **Fig. 2.** Percentage of biodegradable DOC as a function of time. **A**, 'classic' protocol (0.7 μ m
881 GF/F filtration) at 23°C; **B-D**, alternative protocol of 3 μ m - filtered solution incubated at 4°C
882 (B), 23°C (C) and 37°C (D) and filtered through 0.22 μ m at each sampling. The error bars are
883 1 s.d. of triplicates or, in a few cases, duplicates.

884

885

886

887

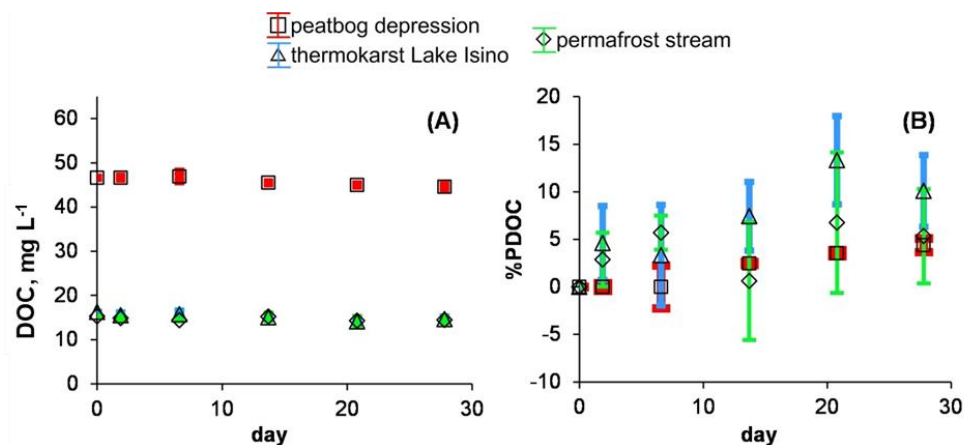
888

889

890



891
892
893



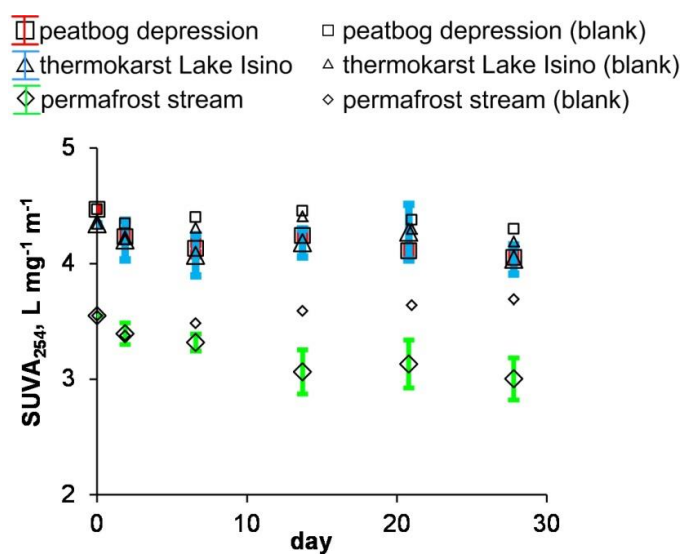
894
895
896

897 **Fig. 3.** Concentration (A) and percentage of degradable (B) DOC in photo-degradation
898 experiments. The experiments are shown by solid symbols and the control runs are shown by
899 open symbols: red squares, peatbog depression; green diamonds, permafrost stream; and
900 triangles, thermokarst Lake Isino. The error bars are 1 s.d. of triplicates.

901
902
903
904
905
906
907
908
909
910
911
912
913
914
915
916



917
918
919
920
921
922
923

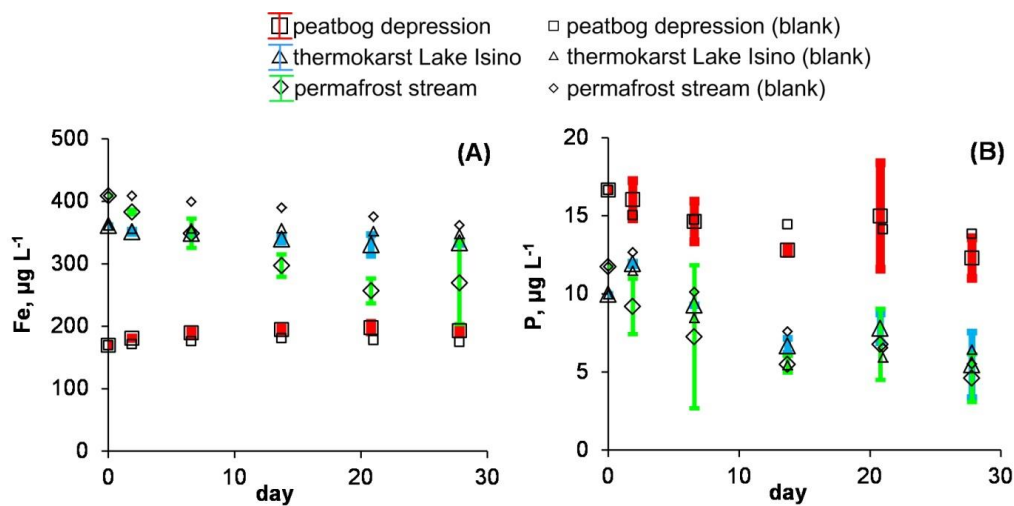


924
925
926
927
928
929
930
931
932
933
934
935
936
937
938
939
940
941
942

Fig. 4. SUVA_{254 nm} over time in photo-degradation experiments. The error bars are 1 s.d. of triplicates.



943
944
945
946
947
948



949
950
951
952
953
954
955
956
957
958
959

Fig. 5. Fe (A) and P (B) concentration over time in photo-degradation experiments. The error bars are 1 s.d. of triplicates.



960 **Table 1.** Landscape setting, hydrochemical characteristics and CO₂ concentration and emission flux of studied waters. S.C. is specific
 961 conductivity.

Sample I.D.	Description	T, °C	pH	S.C., µS cm ⁻¹	DOC, mg L ⁻¹	DIC, mg L ⁻¹	SUVA ₂₅₄	pCO ₂ , ppm	CO ₂ flux, mmol m ⁻² d ⁻¹
BZ-2-17 67°36'48,8"N, 53°54'29,8"E	Depression in peatbog, S _{area} = 7.5 km ²	24	3.85	59.2	43.9	0.992	4.08	440	34
BZ-24-17 , 67°36.53'N 53°50.26'E	Stream in frozen peatland, S _{watershed} = 7.5 km ²	25	6.52	31.5	16.64	2.52	3.32	2370	30-300*
BZ-12 67°36'47,7"N 53°54'38,5"E	Thermokarst lake (Isino), S _{area} = 0.005 km ²	24.1	5.30	12.9	15.65	0.808	4.10	1200	74
P5 67°40'09,4" 52°39'30,8"	r. Pechora, S _{watershed} = 322,000 km ²	20	6.92	65.1	8.20	6.11	3.82	1860 (night) 780 (day)	100-130*

964 Footnote: *, by analogy with small streams of Western Siberian peatlands, of the discontinuous permafrost zone, located in similar
 965 environmental context; ** By analogy with Taz and Pur Rivers of western Siberian peatlands (Serikova et al., 2018).
 966